IEEE Open Journal of Vehicular Technology

Received 19 December 2023; accepted 19 January 2024. Date of publication 8 February 2024;
date of current version 5 March 2024. The review of this article was coordinated by Editor Giambattista Gruosso.

Digital Object Identifier 10.1109/OJVT.2024.3363897

Robust H_∞ Fault-Tolerant Observer-Based PID Path Tracking Control of Autonomous Ground Vehicle With Control Saturation

BOR-SEN CHEN (Life Fellow, IEEE), HAO-TING LIU, AND RUEI-SYUAN WU

Department of Electrical Engineering, National Tsing-Hua University, Hsinchu 30044, Taiwan

CORRESPONDING AUTHOR: BOR-SEN CHEN (e-mail: bschen@ee.nthu.edu.tw)

This article has supplementary downloadable material available at https://doi.org/10.1109/OJVT.2024.3363897, provided by the authors.

ABSTRACT In this study, a robust H_∞ observer-based PID path tracking control strategy is proposed for Autonomous Ground Vehicle (AGV) to efficiently attenuate the effect of external disturbance, actuator/sensor fault signals, and control saturation to achieve the robust path tracking design. To simplify the design procedure, a novel path reference-based feedforward linearization scheme is proposed to transform nonlinear dynamic AGV system to an equivalent linear tracking error system with nonlinear actuator signal. To protect the AGV system from the corruption of actuator/sensor fault signals, two smoothed signal models are introduced to precisely estimate these fault signals to compensate their corruption. Further, the proposed H_∞ fault-tolerant observer-based PID path tracking control strategy of AGV system can be transformed to an equivalent bilinear matrix inequality (BMI). Consequently, by the proposed two-step method, the complex BMI can be transformed into two linear matrix inequalities (LMIs), which can be easily solved via LMI TOOLBOX in MATLAB. Therefore, control restriction is also considered to meet the constraints of physical actuator saturation on PID controller, making the proposed control scheme more applicable. Finally, the triple-lane change task of AGV is simulated as a numerical example to illustrate the design procedure and to validate the performance of proposed design method.

INDEX TERMS AGV, actuator/sensor fault signals, robust observer-based tracking control, linear matrix inequality (LMI), smoothed signal model, fault-tolerant control, PID control, H_∞ tracking control.

I. INTRODUCTION

The autonomous ground vehicle (AGV) has attracted significant attention due to its wide application to intelligent transportation systems [1], [2], [3]. By the implementation of path tracking control, the AGV system can track the desired trajectory while maintaining the stability and precision in path tracking process. Furthermore, the advantages of AGV are manifest in the optimal fuel consumption and improvable on road safety compared to vehicles driven by humans, who often cause accidents due to negligence. Therefore, how to design a path tracking control strategy with low computational resource requirements to achieve the aforementioned advantages of AGV is an important issue.

In brief, the path tracking control is to manipulate an appropriate steering angle and brake/accelerator of AGV, enabling the vehicle to perform desired maneuvers, such as lane changes. The conventional approaches to AGV path tracking control include fuzzy adaptive proportional-integral-derivative (PID) control [4], fuzzy observer-based control [5], [6], [7], nested PID steering control [8], and fuzzy output feedback control [9], etc. However, in spite of the numerous researches on the steering control of AGV, most of them require complex computations to implement the control strategy, such as updating the adaptive law and computing membership function for defuzzification. If the computation can't be done in a timely manner, this issue may lead to a degradation of control performance in practical applications. Furthermore, the saturation of actuators should also be considered for practical reasons.

PID control has been widely and successfully applied in both academia and industry because of its simple structure and easy implementation [10], [11], [12]. A fractional order

proportional integral derivative (FOPID) controller was proposed to control the torques of AGV [13]. An optimally-tuned PID controller is designed for steering control of a four-wheel AGV [14]. A PID longitudinal controller with fuzzy algorithm for AGV was proposed [15]. However, the conventional PID control designs are based on a linearized system model at a specific operation point while the system dynamics of the controlled AGVs are usually nonlinear. Thus, it is necessary to design several sets of PID control gains for each linearized system dynamic model of AGV at different operating points. Even though, the performance of PID control strategy may deteriorate when the system state deviates from the desired operation point. Besides, PID control often involves the need for control gain tuning [16], [17], [18]. The aforementioned two shortages are obstacles encountered in the implementation of PID control of highly nonlinear AGV system.

Since the AGV achieves self-driving capabilities by relying on not only predefined navigation trajectory but also accurate environmental information, the aforementioned results were based on the assumption that the AGV systems were in normal working conditions. Namely, ensuring information accuracy by keeping the control and estimation performance from the influence of fault signals, whose sources may include attack signal through wireless communication channels [19], external disturbance, or system perturbation, is also a crucial concern. In general, the actual systems will inevitably encounter some failures during a long time of operation, which will degrade the estimation and control performance and even cause the systems disastrous consequences [20]. The fault-tolerant control (FTC) design has been considered to have the capacity to ensure the system to maintain an acceptable estimation and control performance when the faults occur [6], [7]. As the result, the fault-tolerant control requires an additional investigation from the control design perspective and has been widely applied despite the existence of protocols developed to protect the data confidentiality [20], [21]. In addition, FTC can be classified into passive FTC and active FTC based on the approach used to handle the fault signal. The former views the fault signal as an unidentified system disturbance and tolerates it with an appropriate control law design. On the other hand, the latter proposes to design an observer that can estimate the fault signal and subsequently incorporates a compensation signal into the feedback controller. Generally, the active FTC has better performance than the passive FTC because of an additional estimation step of fault signal. In the realm of the FTC of AGV system, a virtual actuators-based FTC design is provided to maintain the stability and to avoid the saturation of the actuators [22]. The actuator fault signal can be detected by a model-based fault diagnosis method in [23] and can be eliminated by the disturbance observer-based FTC for electric vehicle [24]. Besides, the trade-off issue between vehicle stability and power consumption in FTC is tackled by the randomized ensemble double $\mathcal{Q}$-learning deep reinforcement learning algorithm [25]. The state estimation problem of AGV system in controller area network with taking into account the impact of fault signal due to saturation effects from wireless communication characteristics is considered in [26]. However, the previous studies often rely on a complicated machine learning or deep learning algorithm in [23], [25] or algebraic equation constraints for designing the fault observer in [24] among the previous researches.

Inspired by the discussion above, the robust H_∞ fault-tolerant observer-based PID path tracking control strategy of AGV system with control saturation under the effect of actuator/sensor fault signal, external disturbance and measurement noise is proposed. In this study, the AGV system is introduced by Newton-Euler equation based on bicycle model. Then, an innovative path reference-based feedforward linearization control method is presented to simplify the nonlinear AGV path tracking system as a linear reference tracking system with an equivalent nonlinear actuator fault signal so that there is no need to use any interpolation-based linearization method to approximate the nonlinearity of AGV system by using a set of locally linearized AGV systems [27]. To deal with the estimation of actuator and sensor fault signal for the compensation of their corruption on the path tracking of AGV system, two smoothed signal models are employed to characterize the dynamic behavior of fault signal systems. By augmenting the AGV system with two smoothed signal models, the Luenberger-type observer can estimate both the state of the AGV system and the fault signal of the actuator/sensor simultaneously. With the help of estimated augmented state, a robust H_∞ fault-tolerant observer-based PID path tracking controller of AGV system under the influence of actuator/sensor fault signal, external disturbance, measurement noise and control saturation can be conducted to fulfill path tracking mission while the negative effect of residue of path reference-based feedforward linearization scheme on the tracking and estimation performance is attenuated below a prescribed attenuation level. Based on the quadratic Lyapunov function, the robust H_∞ fault-tolerant observer-based PID path tracking control design becomes to how to solve a LMI for observer-based PID controller, which can be solved efficiently via MATLAB LMI TOOLBOX with the proposed two-step method. Finally, a numerical simulation example involving the execution of a triple-lane change maneuvering of AGV is provided to illustrate the design procedure and to demonstrate path tracking performance of the proposed H_∞ fault-tolerant observer-based PID controller design of AGV system.

The contributions of this study are outlined below:

1) To simplify the controller design of robust H_∞ fault-tolerant observer-based PID path tracking control of AGV system with control saturation, a path reference-based feedforward linearization control scheme is introduced so that the nonlinear path tracking system of AGV becomes an equivalent linear reference tracking system with an equivalent nonlinear actuator fault signal. Compared with the conventional fuzzy PID methods ([5], [9], [10]), there is no need to interpolate local linearized systems to approximate nonlinear AGV system and therefore the proposal robust

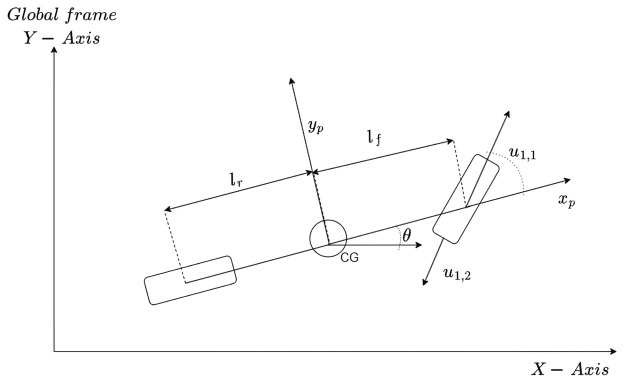

FIGURE 1. Bicycle model for the proposed AGV system.

H_∞ fault-tolerant PID path tracking control scheme significantly reduces the computational complexity of PID control of AGV system for more practical applications.

2) Two smoothed signal models are employed to describe the system dynamic of equivalent actuator/sensor fault signals. Then, the equivalent actuator/sensor fault signals and system states of AGV can be estimated simultaneously by the traditional Luenberger-type observer to compensate for their corruption. Furthermore, with the assistance of the estimated states and fault signals, the robust H_∞ fault-tolerant observer-based PID path tracking controller for the AGV system is constructed to achieve its robust reference path tracking performance while maintaining fault-tolerant capability.
3) The proposed optimal robust H_∞ fault-tolerant observer-based PID path tracking control strategy of AGV system with control saturation can be transformed to an LMIs-constrained optimization problem, which can be easily solved in practice using the proposed two-step method with the help of MATLAB LMI TOOLBOX. Moreover, the PID control gains can be obtained in this design procedure only with a single run and does not need further tuning, thereby reducing the complexity of tuning process of PID parameters in the implementation procedure of conventional PID control schemes [11], [12], [13], [14], [15], [16], [17].

The structure of the remaining study is outlined below. Section II introduces the modeling of the AGV system and the problem formation of the design. Section III presents a robust H_∞ fault-tolerant observer-based PID path tracking control strategy for the AGV system with control saturation by utilizing the Lyapunov function. Section IV provides a numerical simulation example to illustrate the design procedure and to verify the effectiveness of the proposed path tracking method of AGV. Finally, Section V concludes the study.

Notation: A^T: a transpose matrix of A; $A > 0$: a positive definite matrix; $diag(A_1, A_2, \ldots, A_n)$: a block diagonal matrix with aligning the parameter matrices$A_1, A_2, \ldots, A_n$ along the diagonal; $\otimes$: Kronecker product; I_n: n-dimension identity matrix; $x(t) \in L_2[0, t_f]$: if $\int_0^{t_f} x^T(t)x(t)dt < \infty$

II. PRELIMINARY AND PROBLEM FORMULATION

This section provides an introduction to the physical model of the AGV system. Afterward, a feedforward linearization control law is proposed to simplify the observer-based controller design of nonlinear AGV system. Then, two smoothed signal models are utilized to describe the actuator and sensor fault signal to be estimated as compensation signals for active fault-tolerant control. Besides, the robust H_∞ fault-tolerant observer-based PID path tracking control strategy with control saturation is proposed to attenuate the negative effect of unknown environmental noise and fault signals on the path tracking of AGV system.

A. SYSTEM DYNAMIC MODEL OF AUTONOMOUS GROUND VEHICLE

This study presents the physical dynamic of the AGV system based on a bicycle model which considers the system's symmetry relative to the x_p-z plane as shown in Fig. 1, where z direction aligns with $x_p \times y_p$. The dynamic model of AGV system is described as [27]

$$\ddot{x}(t) = M_1(\dot{x}(t))u_1(t) + H_1(\dot{x}(t)) + d_1(t) \tag{1}$$

where $x(t) = [x_p(t) \quad y_p(t) \quad \theta(t)]^T \in \mathbb{R}^3$ represents the state vector of AGV system, which includes longitudinal displacement $x_p(t)$, lateral displacement $y_p(t)$, and yaw angle $\theta(t)$. $d_1(t) = [d_{1x}(t) \quad d_{1y}(t) \quad d_{1\theta}(t)]^T \in \mathbb{R}^3$ denotes the external disturbance with finite energy, $u_1(t) = [u_{1,1}(t) \quad u_{1,2}(t)]^T \in \mathbb{R}^2$ is the control input, where $u_{1,1}(t)$ denotes steering angle of front wheel and $u_{1,2}(t)$ denotes the force applied to brake/accelerator. In addition, the system matrices in (1) are given below:

$$M_1(\dot{x}(t)) = \begin{bmatrix} \frac{2C_{af}(l_f\dot{\theta}(t)+\dot{y}_p(t))}{m\dot{x}_p(t)} & \frac{-2(C_{af}+C_{ar})}{m} \\ \frac{2C_{af}}{m} & 0 \\ \frac{2l_fC_{af}}{I_z} & 0 \end{bmatrix}$$

$$H_1(\dot{x}(t)) = \begin{bmatrix} \dot{y}_p(t)\dot{\theta}(t) \\ h_1(\dot{x}(t)) \\ h_2(\dot{x}(t)) \end{bmatrix}$$

with $h_1(\dot{x}(t)) = -\dot{x}_p(t)\dot{\theta}(t) + \frac{2}{m}(-C_{af}\frac{(l_f\dot{\theta}(t)+\dot{y}_p(t))}{\dot{x}_p} + C_{ar}\frac{(l_r\dot{\theta}(t)-\dot{y}_p(t))}{\dot{x}_p(t)})$ and $h_2(\dot{x}(t)) = \frac{2}{I_z}(l_fC_{af}\frac{(l_f\dot{\theta}(t)+\dot{y}_p(t))}{\dot{x}_p(t)} + l_rC_{ar}\frac{(l_r\dot{\theta}(t)-\dot{y}_p(t))}{\dot{x}_p(t)})$, where C_{af} and C_{ar} are stiffness coefficient of front wheel and rear wheel, respectively, $m \in \mathbb{R}^+$ is the mass, $I_z \in \mathbb{R}^+$ is the moment of inertia, l_f is the length from the front tire to center of gravity (CG) and l_r is the length from the rear tire to CG.

Through appropriate variable transformations and introducing measurement output, (1) can be rewritten as:

$$M\ddot{x}(t) + H(\dot{x}(t)) = u(t) + d(t)$$

$$y(t) = CX(t) + B_2 f_2(t) \tag{2}$$

where

$$M = \begin{bmatrix} m & 0 & 0 \\ 0 & m & 0 \\ 0 & 0 & I_z \end{bmatrix}$$

$$u(t) = \begin{bmatrix} u_x(t) \\ u_y(t) \\ u_\theta(t) \end{bmatrix} = G(\dot{x}(t)) \begin{bmatrix} u_{1,1}(t) \\ u_{1,2}(t) \end{bmatrix} = G(\dot{x}(t)) u_1(t)$$

$$G(\dot{x}(t)) = \begin{bmatrix} \frac{2C_{af}(l_f\dot{\theta}(t)+\dot{y}_p(t))}{\dot{x}_p(t)} & -2(C_{af}+C_{ar}) \\ 2C_{af} & 0 \\ 2l_f C_{af} & 0 \end{bmatrix}$$

$$H(\dot{x}(t)) = \begin{bmatrix} m\dot{y}_p(t)\dot{\theta}(t) \\ mh_1(t) \\ I_z h_2(t) \end{bmatrix}$$

$$d(t) = Md_1(t) = \begin{bmatrix} md_{1x}(t) \\ md_{1y}(t) \\ I_z d_{1\theta}(t) \end{bmatrix}$$

$M \in \mathbb{R}^{3\times 3}$ represents the inertia matrix, $H(\dot{x}(t)) \in \mathbb{R}^3$ stands for the non-inertial force vector, $X(t) = [\int_0^t x^T(\tau)d\tau \quad x^T(t) \quad \dot{x}^T(t)]^T \in \mathbb{R}^9$ is the augmented state vector, $y(t) \in \mathbb{R}^l$ represents the measurement output vector, $C \in \mathbb{R}^{l\times 9}$ is the system measurement matrix, $B_2 \in \mathbb{R}^{l\times p}$ is the system matrix for sensor fault signal and $f_2(t) \in \mathbb{R}^p$ stands for the sensor fault signal and measurement noise.

Remark 1: The integral of the system state, $\int_0^t x^T(\tau)d\tau$, is assumed to be measurable since it can be calculated by an integrator via integrating the information $x(t)$ measured by GPS in practice, i.e., the output $y(t)$ is the measurement of $x(t)$, $\dot{x}(t)$ and $\int_0^t x(\tau)d\tau$. Further, the sensor fault signal $f_2(t)$ can also include measurement noise $n(t)$ in this study.

Remark 2: When $\dot{x}_p(t) \neq 0$, $G(\dot{x}(t))$ has full column rank. Namely, the left inverse matrix of $G(\dot{x}(t))$ exists. If we denote the left inverse matrix of $G(\dot{x}(t))$ as $G_l(\dot{x}(t))$, the actual control input $u_1(t)$ can be computed from $u_1(t) = G_l(\dot{x}(t))u(t)$.

The path reference-based feedforward linearization control law $u(t)$ for AGV system in (2) is designed as follows [28]:

$$u(t) = M(\ddot{r}(t) + u_{PID}(t)) + H(\dot{r}(t)) \tag{3}$$

where $r(t) \in \mathbb{R}^3$ is the path tracking reference, $\ddot{r}(t)$ and $H(\dot{r}(t))$ correspond to the components of the feedforward control mechanism to eliminate the nonlinearity of system, and $u_{PID}(t)$ is PID controller which will be further designed by simple PID control scheme for enhancing robust H_∞ path tracking performance of AGV system.

Afterwards, by substituting the path reference-based feedforward linearization control law $u(t)$ in (3) into (2) and removing $M\ddot{r}(t)$ from both sides, the following reference path tracking error dynamic equation is obtained:

$$\begin{aligned} M(\ddot{x}(t) - \ddot{r}(t)) &= Mu_{PID}(t) - \Delta H(t) + d(t) \\ y(t) &= CX(t) + B_2 f_2(t) \end{aligned} \tag{4}$$

where $\Delta H(t) \triangleq H(\dot{x}(t)) - H(\dot{r}(t))$ is the error term from feedforward linearization. After performing the multiplication M^{-1} on both sides of (4) and making certain adjustment, a reference tracking error equation by feedforward linearized control $u(t)$ is got as follows:

$$\begin{aligned} \ddot{e}(t) &= u_{PID}(t) + f_1(t) \\ y(t) &= CE(t) + CR(t) + B_2 f_2(t) \end{aligned} \tag{5}$$

where $f_1(t) = M^{-1}(-\Delta H(t) + d(t)) \in \mathbb{R}^n$ is viewed as an equivalent actuator fault signal, $e(t) = x(t) - r(t)$ stands for the tracking error, $E(t) = [\int_0^t e^T(\tau)d\tau \quad e^T(t) \quad \dot{e}^T(t)]^T \in \mathbb{R}^9$ and $R(t) = [\int_0^t r^T(\tau)d\tau \quad r^T(t) \quad \dot{r}^T(t)]^T \in \mathbb{R}^9$ are the augmented tracking error vector and the augmented reference path of AGV system, respectively.

Thereafter, the dynamic equation of path tracking error in (5) can be expressed with the following linear state-space error dynamic system:

$$\begin{aligned} \dot{E}(t) &= AE(t) + B(u_{PID}(t) + f_1(t)) \\ y(t) &= CE(t) + CR(t) + B_2 f_2(t) \end{aligned} \tag{6}$$

where $A = \begin{bmatrix} 0 & I_3 & 0 \\ 0 & 0 & I_3 \\ 0 & 0 & 0 \end{bmatrix}$, $B = \begin{bmatrix} 0 \\ 0 \\ I_3 \end{bmatrix}$, and PID control law is of the following form

$$\begin{aligned} u_{PID}(t) &= K_p e(t) + K_I \int_0^t e(\tau)d\tau + K_D \dot{e}(t) \\ &= KE(t) \end{aligned} \tag{7}$$

Remark 3:

i) In the conventional attack-tolerant tracking control of AGV system [5], [27], fuzzy interpolation of several local linear systems is employed to simplify the design procedure of robust attack-tolerant observer-based path tracking control of nonlinear AGV system. However, it needs more design complexity to solve several local linearized attack-tolerant observer-based path tracking problems. Further, it needs more computational time to calculate the fuzzy attack-tolerant observer-based control signal at every time instant [5], [27].

ii) The equivalent actuator fault signal $f_1(t) = M^{-1}(-\Delta H(t) + d(t))$ includes the error term from feedforward linearization compensation and external disturbance, which is a more smoothing signal. The sensor fault signal $f_2(t)$ is mainly due to sensor fault and attack signal.

Remark 4: The displacement and velocity can be measured by sensor in practice, such as gyroscope and GPS. The integrating of displacement can also be obtained by an integrator. Therefore, it is reasonable to implement PID control $u_{PID}(t)$ in this study by augmenting tracking error $e(t)$ with the integrating term $\int_0^t e(\tau)d\tau$ and the differential term $\dot{e}(t)$ as augmented tracking error vector $E(t)$ and design the PID control law as $u_{PID}(t) = KE(t)$, where $K = [K_I \; K_P \; K_D]$.

Based on the derivation above, we convert the path tracking control problem for the nonlinear AGV system with external

disturbance $d(t)$ and $f_2(t)$ in (2) into the stabilization problem of the linear tracking error system under actuator fault signal $f_1(t)$ and sensor fault signal $f_2(t)$ in (6) by the feedforward linearization control law $u(t)$ in (3). Afterward, an adequate PID control law $u_{PID}(t)$ in (7) will be further designed to robustly stabilize this linear tracking error system to achieve path tracking of AGV under fault signals $f_1(t)$ and $f_2(t)$. However, $e(t)$, $\dot{e}(t)$ and $\int_0^t e(\tau)d\tau$ in (6) are unavailable, and only the output $y(t)$ can be measured. Further, actuator fault signal $f_1(t)$ and sensor fault signal $f_2(t)$ will corrupt the PID control $u_{PID}(t)$ and the output measurement $y(t)$, respectively. In this situation, more effort is needed for the observer-based PID path tracking control design of AGV system in (6) and (7).

Remark 5: The row rank of the controllability matrix of the linear tracking error system in (6) is full, i.e, $rank([B, AB, \ldots, A^{9-1}B]) = 9$. Namely, we can stabilize the linear tracking error system in (6) by a proper design PID control $u_{PID}(t)$.

Assumption 2.1: The fault signals $f_1(t)$ and $f_2(t)$ are smooth, which implies there exists the first derivative of both fault signals. Thus, we can describe the first derivative of fault signal $\dot{f}_i(t)$, $i = 1, 2$, by forward difference method

$$\dot{f}_i(t) = \frac{f_i(t+h) - f_i(t)}{h} + R_i(t)$$

where $R_i(t)$ stands for the remainder term and h is the time step.

Remark 6: The actuator fault signal $f_1(t)$ is mainly due to the error from reference-based feedforward linearization and external disturbance and $f_2(t)$ is mainly due to sensor fault signal. Therefore, $f_1(t)$ is more smoothing than the sensor fault signal.

To describe the actuator fault signals $f_1(t)$, the following smoothed signal model is introduced [29]:

$$\begin{aligned} \dot{F}_a(t) &= A_a F_a(t) + v_a(t) \\ f_1(t) &= C_a F_a(t) \end{aligned} \tag{8}$$

where $F_a(t) = [f_1^T(t) \quad f_1^T(t-h) \quad \ldots \quad f_1^T(t-w_a h)]^T \in \mathbb{R}^{3(w_a+1)}$, $v_a(t) = [(\epsilon_1(t) + R_1(t))^T \; R_1^T(t-h) \quad \cdots \; R_1^T(t-w_a h)]^T$ is the approximation error vector of smoothed signal model for actual fault signal, $C_a = [I_3 \quad 0 \quad \ldots \quad 0] \in \mathbb{R}^{3\times 3(w_a+1)}$, w_a is the window size of actuator smoothed signal model, $A_a \in \mathbb{R}^{3(w_a+1)\times 3(w_a+1)}$ is as follows:

$$A_a = \begin{bmatrix} \frac{a_0-1}{h} I_3 & \frac{a_1}{h} I_3 & \cdots & \frac{a_{w_a}}{h} I_3 \\ \frac{1}{h} I_3 & -\frac{1}{h} I_3 & \cdots & 0 \\ 0 & \ddots & & \vdots \\ \vdots & & \ddots & 0 \\ 0 & \cdots & \frac{1}{h} I_3 & -\frac{1}{h} I_3 \end{bmatrix}$$

so that the actuator fault signal of next time step $f_1(t+h)$ can be described by te following extrapolation scheme

$$f_1(t+h) = \sum_{i=0}^{w_a} a_i f_1(t - jh) + \epsilon_1(t) \tag{9}$$

where $\epsilon_1(t)$ is the approximation error of extrapolation for actuator fault signal.

Similar to the formulation of the smoothed signal model conducted on the actuator fault signal $f_1(t)$ in (8), we can establish the following smoothed signal model to describe the sensor fault signal $f_2(t)$:

$$\begin{aligned} \dot{F}_s(t) &= A_s F_s(t) + v_s(t) \\ f_2(t) &= C_s F_s(t) \end{aligned} \tag{10}$$

where $F_s(t) = [f_2^T(t) \quad f_2^T(t-h) \quad \ldots \quad f_2^T(t-w_s h)]^T \in \mathbb{R}^{(w_s+1)\times p}$, $v_s(t) = [(\epsilon_2(t) + R_2(t))^T \; R_2^T(t-h) \quad \cdots \; R_2^T(t-w_s h)]^T$ is the approximation error vector of smoothed signal model for sensor fault signal, $C_s = [I_p \quad 0 \quad \ldots \quad 0] \in \mathbb{R}^{p\times(w_s+1)p}$, w_s is the window size of sensor smoothed signal model and $A_s \in \mathbb{R}^{(w_s+1)p\times(w_s+1)p}$ is as follows

$$A_s = \begin{bmatrix} \frac{b_0-1}{h} I_p & \frac{b_1}{h} I_p & \cdots & \frac{b_{w_s}}{h} I_p \\ \frac{1}{h} I_p & -\frac{1}{h} I_p & \cdots & 0 \\ 0 & \ddots & & \vdots \\ \vdots & & \ddots & 0 \\ 0 & \cdots & \frac{1}{h} I_p & -\frac{1}{h} I_p \end{bmatrix}$$

to describe $f_2(t+h)$ as

$$f_2(t+h) = \sum_{j=0}^{w_s} b_j f_2(t - jh) + \epsilon_2(t) \tag{11}$$

where $\epsilon_2(t)$ is the approximation error of extrapolation for sensor fault signal.

Since A_a, A_s in the smoothed signal model of (8), (10) are fixed constant matrices, there is no need to update the smoothed signal model during maneuvering which saves computation resource and is suitable for practical application. Furthermore, the construction of parameters a_i in (9) and b_j in (11) for the smoothed signal models can be achieved by applying Lagrange extrapolation techniques in [29].

Remark 7: The difference between the proposed smoothed signal models in (8), (10) and other signal models [19], [20], [21], [22], [23], [24], [25], [26] is that, our smoothed signal model decreases the difficulty of model construction by fixing their parameters to avoid frequent parameter estimation during the operation of AGV system. As long as the first derivative of fault signal exists, the proposed signal model is an appropriate design; even if the signal doesn't satisfy with the existence of the first derivative, including the square wave signal, triangle wave signal, stochastic Wiener processes, etc., the proposed robust H_∞ observer-based tracking control strategy can attenuate the effect of approximation errors $v_a(t)$ in

(8) and $v_s(t)$ in (10) of smoothed signal models on estimation and control to the prescribed level in the sequel.

Embedding (8) and (10) into (6), we get the following augmented tracking error system of AGV:

$$\dot{\bar{E}}(t) = \bar{A}\bar{E}(t) + \bar{B}u_{PID}(t) + \bar{v}(t)$$
$$y(t) = \bar{C}\bar{E}(t) + CR(t) \tag{12}$$

where $\bar{E}(t) = \begin{bmatrix} E(t) \\ F_a(t) \\ F_s(t) \end{bmatrix}$ is the augmented tracking error vector, $\bar{A} = \begin{bmatrix} A & BC_a & 0 \\ 0 & A_a & 0 \\ 0 & 0 & A_s \end{bmatrix}$, $\bar{B} = \begin{bmatrix} B \\ 0 \\ 0 \end{bmatrix}$, $\bar{C} = [C \quad 0 \quad B_2C_s]$, and $\bar{v}(t) = \begin{bmatrix} 0 \\ v_a(t) \\ v_s(t) \end{bmatrix}$.

Through augmenting smoothed signal models with the tracking error system, it becomes possible to prevent the augmented tracking error system in (12) from the impact of the fault signals $f_1(t)$ and $f_2(t)$. Namely, the tracking error in (6) is protected against the corruption of fault signals $f_1(t)$ and $f_2(t)$. By utilizing the augmented system in (12), a Luenberger-type observer can be employed as the following form to estimate the state of the augmented tracking error system $e(t)$ and fault signals $f_1(t)$, $f_2(t)$, simultaneously.

$$\text{where } \dot{\hat{\bar{E}}}(t) = \bar{A}\hat{\bar{E}}(t) + \bar{B}u_{PID}(t) - L(y(t) - \hat{y}(t))$$
$$\hat{y}(t) = \bar{C}\hat{\bar{E}}(t) + CR(t) \tag{13}$$

Assumption 2.2: The augmented tracking error system in (12) is observable [29], i.e., $rank\begin{bmatrix} zI - \bar{A} \\ \bar{C} \end{bmatrix} = 9 + 3(w_a + 1) + (w_s + 1)p, \ \forall z \in eig(\bar{A})$.

Remark 8 The selection of coefficients $a_0, \ldots, a_{w_a}$ of A_a in (8) and $b_0, \ldots, b_{w_s}$ of A_s in (10) must be satisfied with the observability condition in Assumption 2.2. In general, if $a_0, \ldots, a_{w_a}$ and $b_0, \ldots, b_{w_s}$ are selected so that A_a and A_s have not same eigenvalues, then the observability of the augmented tracking error system in (12) can be guaranteed [29].

By utilizing the estimated augmented state in (13) which contains the augmented estimated tracking error vector and actuator/sensor estimated fault signal, the observer-based PID control law $u_{PID}(t)$ in (7) can be redesigned as follows:

$$u_{PID}(t) = \bar{K}\hat{\bar{E}}(t) \tag{14}$$

where $\bar{K}$ contains the PID control gains.

Remark 9: By defining the augmented observer-based PID control $u_{PID}(t) = \bar{K}\hat{\bar{E}}(t) = [K \ K_{F_a} \ K_{F_s}] \times [\hat{E}^T(t) \ \hat{F}_a^T(t) \ \hat{F}_s^T(t)]^T = K\hat{E}(t) + K_{F_a}\hat{F}_a(t) + K_{F_s}\hat{F}_s(t)$, it can be seen that the feedback control gain $\bar{K}$ is the combination of the PID control gains K for $\hat{E}(t)$, along with the active fault-tolerant control gains K_{F_a} and K_{F_s} for $\hat{F}_a(t)$ and $\hat{F}_s(t)$ to compensate the effect of actuator/sensor fault signals $f_1(t)$ and $f_2(t)$ in (6) on the path tracking control and the path estimation of AGV system, respectively. This implies the new design for observer-based PID controller $u_{PID}(t)$ has FTC ability.

To design the observer gain L in (13), we introduce a new variable $\tilde{E}(t) = \bar{E}(t) - \hat{\bar{E}}(t)$ to represent the augmented state estimation error, and the corresponding augmented estimation error dynamic system can be described based on (12) and (13):

$$\dot{\tilde{E}}(t) = \bar{A}\tilde{E}(t) + L\bar{C}\tilde{E}(t) + \bar{v}(t) \tag{15}$$

Combining (12), (14), and (15), the tracking error system of AGV in (12) with the observer-based PID control design in (13) and (14) can be combined with the estimation error dynamic system in (15) as follows:

$$\dot{\tilde{x}}(t) = \tilde{A}\tilde{x}(t) + \tilde{v}(t) \tag{16}$$

where $\tilde{x}(t) = \begin{bmatrix} \bar{E}(t) \\ \tilde{E}(t) \end{bmatrix}$, $\tilde{A} = \begin{bmatrix} \bar{A} + \bar{B}\bar{K} & -\bar{B}\bar{K} \\ 0 & \bar{A} + L\bar{C} \end{bmatrix}$, and $\tilde{v}(t) = \begin{bmatrix} \bar{v}(t) \\ \bar{v}(t) \end{bmatrix}$

B. PROBLEM FORMULATION

Therefore, the fault-tolerant observer-based PID path tracking control design procedure of AGV system becomes how to specify control gain $\bar{K}$ in (14) and observer gain L in (13) to achieve the robust stabilization problem under external disturbance $\tilde{v}(t)$ in (16). Since $\tilde{v}(t)$ in (16) is unavailable, the effect of $\tilde{v}(t) \in L_2[0, t_f]$ should be taken into consideration when we design $\bar{K}$ and L of the observer-based PID controller in (13) and (14). Hence, in this study, the following robust H_∞ fault-tolerant observer-based PID path tracking control strategy is proposed with a prescribed attenuation level ρ for AGV system:

$$J = \frac{\int_0^{t_f} (\bar{E}^T(t)\bar{Q}\bar{E}(t) + \tilde{E}^T(t)\tilde{Q}\tilde{E}(t) + u_{PID}^T(t)Ru_{PID}(t))dt - V(\tilde{x}(0))}{\int_0^{t_f} \tilde{v}^T(t)\tilde{v}(t)dt} \le \rho^2$$
$$\forall \ \tilde{v}(t) \in L_2[0, t_f] \tag{17}$$

where t_f is the terminal time, $\{\bar{Q}, \ \tilde{Q}, \ R\}$ are the positive definite weighting matrices on the tracking error, estimation error, feedback control input, respectively. $V(\tilde{x}(0))$ denotes the initial condition effect of the augmented tracking and estimation error system in (16), which needs to be extracted in the H_∞ observer-based PID control performance, and $\tilde{v}(t)$ represents the possible disturbance whose effect is necessary to be attenuated on $\bar{E}(t)$, $\tilde{E}(t)$, and $u_{PID}(t)$. The physical meaning of the robust H_∞ observer-based PID control strategy in (17) is that from the energy perspective, the effect of the approximation error $\tilde{v}(t) \in L_2[0, t_f]$ of proposed smoothed signal model on the augmented tracking error $\bar{E}(t)$, augmented estimation error $\tilde{E}(t)$ and PID control input $u_{PID}(t)$ must be attenuated below a predefined attenuation level ρ^2, i.e., the PID control gain $\bar{K}$ in (14) and observer gain L in (13) must be specified to satisfy the desired robust H_∞ fault-tolerant observer-based PID path tracking performance in (17).

III. ROBUST H_∞ FAULT-TOLERANT OBSERVER-BASED PID PATH TRACKING CONTROL STRATEGY FOR AGV SYSTEM WITH CONTROL SATURATION

To facilitate the design of the robust H_∞ fault-tolerant observer-based PID path tracking control strategy in (17), the following lemmas are provided before further analysis:

Lemma 1: For any matrices X and Y with proper dimensions and positive definite matrix S, the inequality stated below is valid [30]:

$$X^TY + Y^TX \le X^TSX + Y^TS^{-1}Y \tag{18}$$

Lemma 2 (Schur Complement): For the symmetric matrices X, Y and matrix S with proper dimensions, the following statement is equivalent [30]:

$$Y > 0,\ X - SY^{-1}S^T > 0 \Leftrightarrow \begin{bmatrix} X & S \\ S^T & Y \end{bmatrix} > 0 \tag{19}$$

With the help of Lyapunov function, the design of proposed observer-based PID path tracking control for AGV system can be transformed to an equivalent linear matrix inequality (LMI) in the following theorem.

Theorem 1: (i) If there exists matrices $P = P^T > 0, \bar{K}, L$ such that the following bilinear matrix inequality (BMI) holds:

$$Q + P\tilde{A} + \tilde{A}^TP + \tilde{K}^TR\tilde{K} + \frac{1}{\rho^2}PP \le 0 \tag{20}$$

where $\tilde{K} = \begin{bmatrix} \bar{K} & -\bar{K} \end{bmatrix}$, $Q = \begin{bmatrix} \bar{Q} & 0 \\ 0 & \tilde{Q} \end{bmatrix}$, then the robust H_∞ fault-tolerant observer-based PID path tracking control strategy in (17) is guaranteed for a prescribed attenuation level ρ^2. (ii) If $\bar{v}(t) \in L_2[0,\infty)$, i.e., $\bar{v}(t)$ is of finite energy, then $\tilde{E}(t) \to 0$ and $\bar{E}(t) \to 0$ as $t \to \infty$, i.e., the asymptotical estimation and tracking are all achieved as $t \to \infty$ by the proposed robust H_∞ fault-tolerant observer-based PID path tracking control strategy.

Proof: (i) For the augmented system (16), we define a quadratic Lyapunov function $V(\tilde{x}(t)) = \tilde{x}^T(t)P\tilde{x}(t)$ where P is a positive definite matrix to be solved.

$$\begin{aligned}
&\int_0^{t_f} (\tilde{x}^T(t)Q\tilde{x}(t) + u_{PID}^T(t)Ru_{PID}(t))dt \\
&= -(V(\tilde{x}(t_f)) - V(\tilde{x}(0))) + \int_0^{t_f} (\tilde{x}^T(t)Q\tilde{x}(t) \\
&\quad + u_{PID}^T(t)Ru_{PID}(t) + \dot{V}(\tilde{x}(t)))dt \\
&\le V(\tilde{x}(0)) + \int_0^{t_f} (\tilde{x}^T(t)Q\tilde{x}(t) \\
&\quad + u_{PID}^T(t)Ru_{PID}(t) + \dot{\tilde{x}}^T(t)P\tilde{x}(t) + \tilde{x}^T(t)P\dot{\tilde{x}})dt
\end{aligned} \tag{21}$$

By (16) and Lemma 1 with $S = \rho^2 I$, we get:

$$\begin{aligned}
&\dot{\tilde{x}}^T(t)P\tilde{x}(t) + \tilde{x}^T(t)P\dot{\tilde{x}} \\
&= (\tilde{A}\tilde{x}(t) + \tilde{v}(t))^TP\tilde{x}(t) + \tilde{x}^T(t)P(\tilde{A}\tilde{x}(t) + \tilde{v}(t)) \\
&\le \tilde{x}^T(t)\left(P\tilde{A} + \tilde{A}^TP + \frac{1}{\rho^2}PP\right)\tilde{x}(t) + \rho^2\tilde{v}^T(t)\tilde{v}(t)
\end{aligned} \tag{22}$$

Substituting (14) and (22) into (21), we get:

$$\begin{aligned}
&\int_0^{t_f} (\tilde{x}^T(t)Q\tilde{x}(t) + u_{PID}^T(t)Ru_{PID}(t))dt \\
&\le V(\tilde{x}(0)) + \int_0^{t_f} \left(\tilde{x}^T(t)\left(Q + P\tilde{A} + \tilde{A}^TP + \tilde{K}^TR\tilde{K}\right.\right. \\
&\quad \left.\left. + \frac{1}{\rho^2}PP\right)\tilde{x}(t) + \rho^2\tilde{v}^T(t)\tilde{v}(t)\right)dt
\end{aligned} \tag{23}$$

From (20) and $\tilde{x}^TQ\tilde{x} = \bar{E}^T\bar{Q}\bar{E} + \tilde{E}^T\tilde{Q}\tilde{E}$, we get

$$\begin{aligned}
&\int_0^{t_f} (\tilde{x}^T(t)Q\tilde{x}(t) + u_{PID}^T(t)Ru_{PID}(t))dt \\
&= \int_0^{t_f} (\bar{E}^T(t)\bar{Q}\bar{E}(t) + \tilde{E}^T\tilde{Q}\tilde{E} + u_{PID}^T(t)Ru_{PID}(t))dt \\
&\le V(\tilde{x}(0)) + \rho^2\int_0^{t_f} (\tilde{v}^T(t)\tilde{v}(t))dt
\end{aligned} \tag{24}$$

Therefore, the H_∞ control performance in (17) is achieved with a prescribed ρ^2.

(ii) If $\bar{v}(t) \in L_2[0,\infty)$, then $\int_0^\infty \bar{v}^T(t)\bar{v}(t)dt < \infty$. Then, from (24), since $V(\tilde{x}(0)) < \infty$, we get $\int_0^\infty \bar{E}^T(t)\bar{Q}\bar{E}(t) + \tilde{E}^T(t)\tilde{Q}\tilde{E}(t) + u_{PID}^T(t)Ru_{PID}(t)dt < \infty$, i.e. $\bar{E}(t) \to 0$, $\tilde{E}(t) \to 0$ and $u_{PID}(t) \to 0$ as $t \to \infty$, Q.E.D. ■

However, the existence of the strong coupling effect between the designed variables $\bar{K}$ and L in the BMI in (20) leads to the ineffectiveness of solving these two variables. Fortunately, we can tackle this issue by a two-step design method outlined below:

Step 1: Since the augmented system in (16) is composed of two subsystems in (12) and (15), the Lyapunov(energy) function consists of two Lyapunov functions of subsystems, i.e. $V(\tilde{x}(t)) = \tilde{x}^T(t)P\tilde{x}(t) = \bar{E}^T(t)\bar{P}\bar{E}(t) + \tilde{E}^T(t)\tilde{P}\tilde{E}(t)$ with $P = \begin{bmatrix} \bar{P} & 0 \\ 0 & \tilde{P} \end{bmatrix}$. Therefore, replacing Q in (20) with $\begin{bmatrix} \bar{Q} & 0 \\ 0 & \tilde{Q} \end{bmatrix}$, we obtain

$$\begin{aligned}
&\begin{bmatrix} \bar{Q} & 0 \\ 0 & \tilde{Q} \end{bmatrix} + \begin{bmatrix} \bar{P} & 0 \\ 0 & \tilde{P} \end{bmatrix}\begin{bmatrix} \bar{A} + \bar{B}\bar{K} & -\bar{B}\bar{K} \\ 0 & \bar{A} + L\bar{C} \end{bmatrix} \\
&\quad + \left(\begin{bmatrix} \bar{P} & 0 \\ 0 & \tilde{P} \end{bmatrix}\begin{bmatrix} \bar{A} + \bar{B}\bar{K} & -\bar{B}\bar{K} \\ 0 & \bar{A} + L\bar{C} \end{bmatrix}\right)^T \\
&\quad + \begin{bmatrix} \bar{K}^TR\bar{K} & -\bar{K}^TR\bar{K} \\ -\bar{K}^TR\bar{K} & \bar{K}^TR\bar{K} \end{bmatrix} + \frac{1}{\rho^2}\begin{bmatrix} \bar{P}\bar{P} & 0 \\ 0 & \tilde{P}\tilde{P} \end{bmatrix} \\
&= \begin{bmatrix} M_{11} & M_{12} \\ M_{12}^T & M_{22} \end{bmatrix} < 0
\end{aligned} \tag{25}$$

where $M_{11} = \bar{Q} + \bar{P}(\bar{A} + \bar{B}\bar{K}) + (\bar{P}(\bar{A} + \bar{B}\bar{K}))^T + \bar{K}^TR\bar{K} + \frac{1}{\rho^2}\bar{P}\bar{P}$, $M_{22} = \tilde{Q} + \tilde{P}(\bar{A} + L\bar{C}) + (\tilde{P}(\bar{A} + L\bar{C}))^T + \bar{K}^TR\bar{K} + \frac{1}{\rho^2}\tilde{P}\tilde{P}$, $M_{12} = -\bar{P}\bar{B}\bar{K} - \bar{K}^TR\bar{K}$, which are still bilinear matrices of design parameters $\bar{P}$, $\tilde{P}$, $\bar{K}$, and L. Therefore, it is not easy to solve BMI in (25) for $\bar{P}$, $\tilde{P}$, $\bar{K}$, and L. By the fact that [30]

$$\begin{bmatrix} M_{11} & M_{12} \\ M_{12}^T & M_{22} \end{bmatrix} < 0 \Rightarrow M_{11} < 0, M_{22} < 0$$

we can solve the inequality $M_{11} < 0$ at first to get $\bar{P}, \bar{K}$.

Thus, we define $\bar{W} = \bar{P}^{-1}$ and multiply it on the both sides of $M_{11} < 0$. After utilizing Schur complement in Lemma 2 two times, we can get the following LMI:

$$\begin{bmatrix} \bar{M}_{11} + \frac{1}{\rho^2} & \bar{W}\sqrt[1/2]{\bar{Q}} & \bar{Y}^T \\ \left(\bar{W}\sqrt[1/2]{\bar{Q}}\right)^T & -I & 0 \\ \bar{Y} & 0 & -R^{-1} \end{bmatrix} < 0 \tag{26}$$

where $\bar{M}_{11} = \bar{A}\bar{W} + \bar{B}\bar{Y} + (\bar{A}\bar{W} + \bar{B}\bar{Y})^T$, $\bar{Y} = \bar{K}\bar{W}$. By solving the LMI in (26), $\bar{W}$ and $\bar{Y}$ can be obtained and then $\bar{K} = \bar{Y}\bar{W}^{-1}$ can be get.

Step 2: Substituting $\bar{P} = \bar{W}^{-1}$ and $\bar{K} = \bar{Y}\bar{W}^{-1}$ in *Step 1* into (25) and applying Lemma 2, the following LMI can be got:

$$\begin{bmatrix} M_{11} & M_{12} & 0 \\ M_{12}^T & \tilde{Q} + \tilde{M}_{22} + \bar{K}^T R \bar{K} & \tilde{P} \\ 0 & \tilde{P}^T & -\rho^2 I \end{bmatrix} < 0 \tag{27}$$

where $\tilde{M}_{22} = \tilde{P}\bar{A} + \tilde{Y}\bar{C} + (\tilde{P}\bar{A} + \tilde{Y}\bar{C})^T$, $\tilde{Y} = \tilde{P}L$. Therefore, $\tilde{P}$ and $L = \tilde{P}^{-1}\tilde{Y}$ can be obtained by solving the LMI in (27).

Remark 10: Since the proof procedure of Theorem 1 is derived by a series of inequalities, the solution of two-step design with the corresponding attenuation level ρ will be conservative. Nevertheless, the performance of proposed H_∞ fault-tolerant observer-based PID path tracking control strategy would be better in practice generally.

Furthermore, due to the integration phenomenon of PID control signal, the control saturation is always concerned in PID control design since control input limit inevitably exists and is restricted by physical saturation of actuator in the practical application of AGV. Suppose that $\bar{E}(t)$ is restricted to stay in an invariant ellipsoid $\varepsilon_r = \{\bar{E}(t) \in \mathbb{R}^{(9+3(w_a+1)+(w_s+1)p)} | \bar{E}^T(t)\bar{W}^{-1}\bar{E}(t) \le 1\}$ for $t \ge 0$, and if $\nu^2\bar{W}^{-1} \ge \bar{K}^T\bar{K}$ for $\nu \in \mathbb{R}^+$, then we can obtain [31]

$$\begin{aligned} &\max_{t\ge 0} \ \|u_{PID}(t)\|_2 \\ &= \max_{t\ge 0} \ \|\bar{K}\bar{E}(t)\|_2 \\ &\le \max_{\bar{E}\in\varepsilon_r} \ \|\bar{K}\bar{E}(t)\|_2 \\ &\le \max_{\bar{E}\in\varepsilon_r} \ \|\nu\bar{W}^{-\frac{1}{2}}\bar{E}(t)\|_2 \\ &= \max_{\bar{E}\in\varepsilon_r} \ \sqrt{\nu^2\bar{E}^T(t)\bar{W}^{-1}\bar{E}(t)} \\ &\le \nu \end{aligned}$$

Namely, $\|u_{PID}(t)\|_2 \le \nu$ if $\nu^2\bar{W}^{-1} \ge \bar{K}^T(t)\bar{K}(t)$ holds or $\nu^2\bar{W} \ge (\bar{K}\bar{W})^T\bar{K}\bar{W} = \bar{Y}^T\bar{Y}$ holds for $t \ge 0$. Therefore, by Schur complement in Lemma 2, the above constraint is equivalent to the following LMI

$$\begin{bmatrix} \nu^2\bar{W} & \bar{Y}^T \\ \bar{Y} & I_3 \end{bmatrix} \ge 0 \tag{28}$$

i.e., if the LMI constraint in (28) holds to ν, then the amplitude of PID control signal is limited by $\|u_{PID}(t)\|_2 \le \nu$ of actuator saturation.

Therefore, the optimal robust H_∞ fault-tolerant observer-based PID path tracking control strategy with control saturation for AGV systems can be solved by the following LMIs-constrained optimization problem:

$$\begin{aligned} \rho^{*2} = &\min_{\bar{W}>0,\ \bar{K},\ L} \rho^2 \\ &\text{subject to (26), (27), (28)} \end{aligned} \tag{29}$$

With the help of LMI TOOLBOX in MATLAB, the above LMIs-constrained optimal problem can be solved for PID control gain $K^* = [K_P^* K_I^* K_D^*]$ and observer gain L^* by decreasing the attenuation level ρ^2 until there exists no positive solution $\bar{W} > 0$ for (26), (27) and (28).

Remark 11: In conventional PID control designs, designers need to tune these PID control parameters to achieve some design purposes, which are always very complicated and difficult tunning processes. In this study, the PID control parameters $[K_P^* K_I^* K_D^*]$ and observer gain L^* can be obtained by solving the LMIs-constrained optimization problem (29) by decreasing ρ^2 in a single run with the help of LMI TOOLBOX in MATLAB.

Consequently, the design procedure of the optimal robust H_∞ fault-tolerant observer-based PID path tracking control for AGV system in (2) is summarized as follows:

1) Implement the path reference-based feedforward control scheme in (3) to derive the linearized dynamic system of the tracking error equation in (5) for the AGV system.
2) Construct the parameters a_i in (9) and b_j in (11) for the smoothed signal models in (8) and (10) while checking the rank condition for observability of the augmented tracking error system in (12) in Assumption 2.2 to achieve the active FTC capability for actuator fault signal $f_1(t)$ and sensor fault signal $f_2(t)$, respectively.
3) Obtain the augmented tracking error system in (12) by embedding two smoothed signal models into the linearized system in (6).
4) Determine the weighting matrices $\bar{Q} \ge 0, \tilde{Q} \ge 0, R > 0$ and the upper bound of the PID control input ν for the robust H_∞ fault-tolerant observer-based PID path tracking control strategy in (17) with control saturation in (28) according to the desired design goal.
5) By the proposed two-step design procedure, find the optimal PID control gain $\bar{K}^*$ and optimal observer gain L^* for the observer-based PID controller in (13) and (14) through the solution of the LMIs-constrained optimization problem in (29).
6) Construct path reference-based feedforward linearization control law $u(t)$ in (3) to get the actual control input $u_1(t)$ from $u_1(t) = G_l(\dot{\hat{x}}(t))u(t)$.

The procedure of above optimal H_∞ fault-tolerant observer-based PID path tracking control strategy of AGV can be

designed in Algorithm 1 for more practical applications. Unlike the complicated tuning process of conventional PID control design methods, the proposed PID controller can be obtained in a single run.

IV. SIMULATION EXAMPLE

To meet the requirements of the smart city application, the AGV system should be able to track a reference trajectory to complete some specific mission. However, the negative effect from actuator/sensor fault signal and external disturbance is inevitable. Therefore, these negative influences are considered in this simulation to validate the effectiveness of the proposed robust path reference tracking control method of AGV system.

A. STRUCTURE OF SYSTEMS

In this section, the AGV system in (1) has to accomplish a triple-lane change task to demonstrate a scenario for a vehicle switches lanes for both overtaking and avoiding obstacles while maneuvering. In the observer-based PID control strategy of AGV system in (6), the position and speed variables are available by GPS and gyroscope and the integral term $\int_0^t x^T(\tau)d\tau$ can be obtained by an integrator, so that it is reasonable to choose an identity matrix I_9 as measurement output matrix C in (6). The remainders of system parameters and design parameters are specified as the subsequent arrangement:

1) *AGV system parameters [5]:* $m = 1530\,(\text{kg})$, $I_z = 4607\,(\text{kg}\cdot\text{m}^2)$, $C_{af} = 9.5\times10^4\,(\text{N/rad})$, $C_{ar} = 8.55\times10^4\,(\text{N/rad})$, $l_f = 1.11\,(\text{m})$, $l_r = 1.67\,(\text{m})$.
2) *Design parameters:* Initial $\rho = 100$, $\rho_s = 0.01$, $w_a = 3$ and $w_s = 2$, $a_0 = 0.9$, $a_1 = 0.01$, $a_2 = 0.01$, $a_3 = 0.002$, $b_0 = 0.9$, $b_1 = 0.09$, $b_2 = 0.001$, $\bar{Q} = diag(\bar{Q}_1, 0, 0)$ where $\bar{Q}_1 = diag(0.001, 0.01, 30)\otimes I_3$, $\tilde{Q} = 20\times diag(\tilde{Q}_1, \tilde{Q}_2, \tilde{Q}_3)$ where $\tilde{Q}_1 = diag(0.01, 0.01, 1)\otimes I_3$, $\tilde{Q}_2 = diag(1, 0.1, 0.01, 0.001)\otimes I_3$, $\tilde{Q}_3 = diag(1, 0.1, 0.01)\otimes I_p$, p = 9, h = 0.001, $\nu = 10$.
3) *External influence:* $d(t) = 5\times[\sin(t)\ \sin(t)\ \sin(t)]^T + 0.5\times[\sin(5t)\ \sin(5t)\ \sin(5t)]^T$, $f_2(t)$ is set as a square wave with amplitude 0.25 and frequency 0.1 Hz.
4) *Initial condition:* $\tilde{x}(0) = [E(0)^T, F_a(0)^T, F_s(0)^T, \tilde{E}(0)^T] = [[0.1\ 0.2\ 0.1\ 0.1\ 0.2\ 0.1\ 0\ 0\ 0\ ]^T, \mathbf{0}, \mathbf{0}, [0.1\ 0.2\ 0.1\ 0.1\ 0.2\ 0.1\ 0\ 0\ 0\ ]]^T$, where $\mathbf{0}$ denotes the zero matrix with the corresponding dimension.

B. SIMULATION RESULTS

At first, the optimal control gain $\bar{K}^*$ and the optimal observer gain L^* of the optimal robust H_∞ fault-tolerant observer-based PID path reference tracking control strategy are obtained with the optimal attenuation level $\rho^* = 43.27$ in (29) by the proposed design procedure in Algorithm 1 with the above design parameters.

To evaluate the reference path tracking performance of AGV system by the proposed optimal H_∞ fault-tolerant observer-based PID reference path tracking control strategy in future smart city, a triple-lane change task is conducted and

Algorithm 1: Design Procedure of Optimal Robust H_∞ Fault-Tolerant Observer-Based PID Path Tracking Control strategy of AGV System With Control Saturation.

Input: Smoothed signal model parameters a_i, b_j; weighting matrix $\bar{Q}\geq 0$, $\tilde{Q}\geq 0$, $R>0$; upper bound of the PID control input ν; initial ρ; decreasing step ρ_s;

Output: Optimal control gain $\bar{K}^*$, optimal observer gain L^* and optimal attenuation level ρ^*

Initialize $IfSolved \leftarrow false$; /* If can be solved. */
if *rank in Assumption 2.2 holds* **then**
  /* Solve optimal LMIs problem */
  Initialize $If\ Optimal \leftarrow false$; /* If optimal solution. */
  while *not* $IfOptimal$ **do**
    /* Step 1 */
    Solve (26) and (28) simultaneously to get $\bar{P} = \bar{W}^{-1}$ and $\bar{K} = \bar{Y}\bar{W}^{-1}$.;
    $m_1 \leftarrow \begin{bmatrix} \bar{M}_{11} + \frac{1}{\rho^2} & \bar{W} & \sqrt[1/2]{\bar{Q}} & \bar{Y}^T \\ (\bar{W}\sqrt[1/2]{\bar{Q}})^T & -I & 0 \\ \bar{Y} & 0 & -R^{-1} \end{bmatrix}$;
    $m_2 \leftarrow \begin{bmatrix} \nu^2\bar{W} & \bar{Y}^T \\ \bar{Y} & I_3 \end{bmatrix}$;
    $check_1 \leftarrow \bar{P} > 0\ and\ m_1 < 0\ and\ m_2 \geq 0$;
    if $check_1$ **then**
      /* Step 2 */
      Solve (27) to get $\tilde{P}$ and $L = \tilde{P}^{-1}\tilde{Y}$;
      $m_3 \leftarrow \begin{bmatrix} M_{11} & M_{12} & \tilde{P} \\ M_{12}^T & \tilde{Q} + \tilde{M}_{22} + \bar{K}^T R\bar{K} & 0 \\ \tilde{P}^T & 0 \end{bmatrix}$;
      $check_2 \leftarrow \tilde{P} > 0\ and\ m_3 < 0$;
      if $check_2$ **then**
        /* Update optimal solution */
        $\bar{K}^* \leftarrow \bar{K}$; $L^* \leftarrow L$; $\rho^* \leftarrow \rho$;
        $IfSolved \leftarrow true$
        $\rho \leftarrow \rho - \rho_s$
      else
        if $IfSolved$ **then**
          $IfOptimal \leftarrow true$
        else
          /* No proper solution, redesign. */
        end if
      end if
    else
      if $IfSolved$ **then**
        $IfOptimal \leftarrow true$
      else
        /*No proper solution, redesign. */
      end if
    end if
  end while
else
  /* Smoothed signal models are unobservable, redesign a_i, b_j */
end if

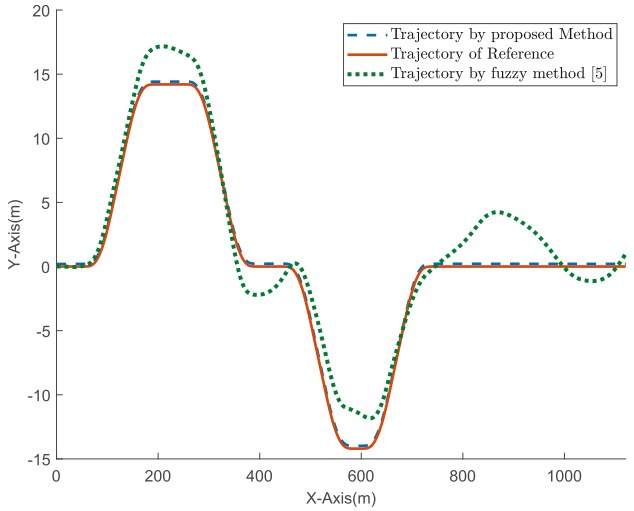

FIGURE 2. Path reference tracking performance of triple-lane change task in the 2-D graph of AGV during the maneuvering process by the proposed method and fuzzy method in [5].

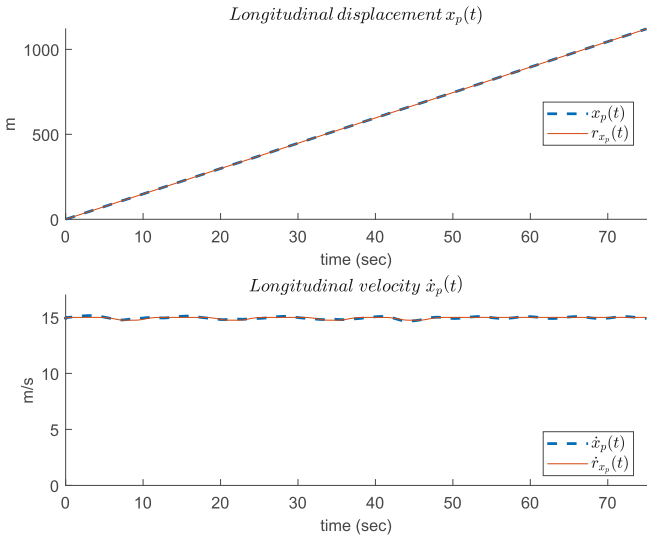

FIGURE 3. Tracking performance of longitudinal displacement $x_p(t)$ and longitudinal velocity $\dot{x}_p(t)$ of AGV system by the proposed method.

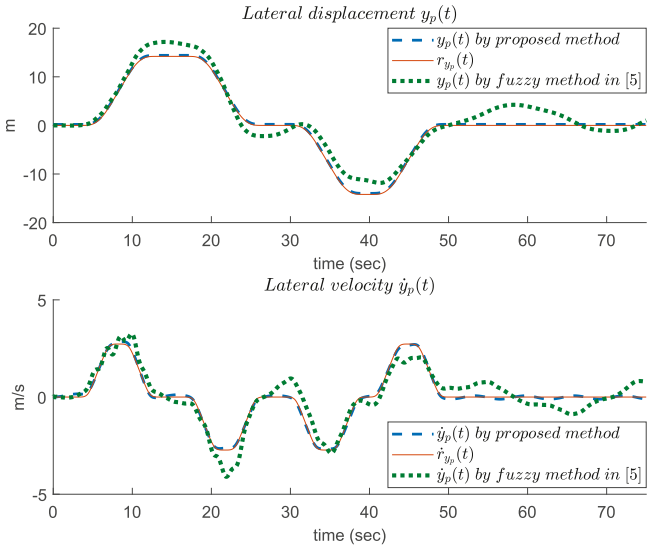

FIGURE 4. Tracking performance of lateral displacement $y_p(t)$ and lateral velocity $\dot{y}_p(t)$ of AGV system by the proposed method and the fuzzy method [5].

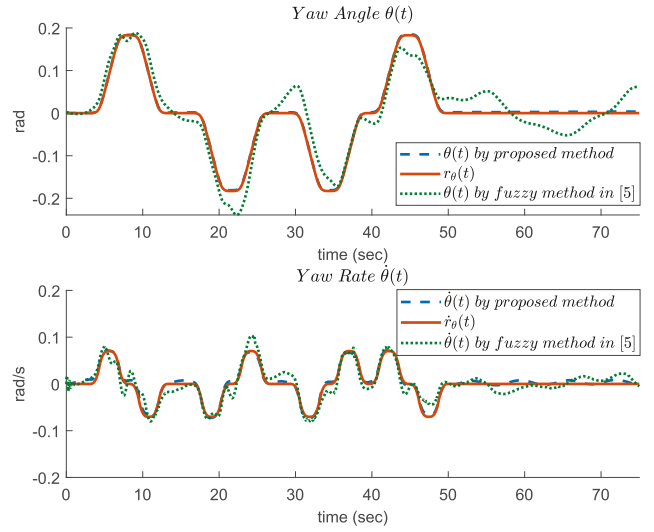

FIGURE 5. Tracking performance of yaw angle $\theta(t)$ and yaw rate $\dot{\theta}(t)$ of AGV system by the proposed method and the fuzzy method [5].

presented in Fig. 2. This reference path not only stands for the lane change but also represents the obstacle avoidance. Thereafter, each reference path tracking performance of the AGV system by the proposed method in comparison with the robust fuzzy method in [5] are depicted in Figs. 4 and 5 to validate the effectiveness of the proposed method. However, it should be noted that in the fuzzy method, the longitudinal displacement $x_p(t)$ and longitudinal velocity $\dot{x}_p(t)$ are not considered into dynamic model in (1) for path tracking of AGV system. As a result, these reference path tracking result are not included and are assumed to be the same as reference signals in Fig. 3. In this triple-lane change task, except for slight deceleration during turning at about 4 s, 18 s, 30 s, and 41 s, the longitudinal velocity $\dot{x}_p(t)$ maintains a constant speed of 15 m/s for the rest of the time. Therefore, the variation of the yaw angle $\theta(t)$ is controlled within a small angle range, which can prevent the AGV from getting out of control due to abrupt turns in such velocity. Furthermore, the lateral displacement $y_p(t)$ is highly correlated with the yaw angle $\theta(t)$. Analyzing the AGV system dynamics in (1), it can be found that the influence from actual control input $u_1(t)$ on $\ddot{y}_p(t)$ and $\ddot{\theta}(t)$ is proportional to a factor of $\frac{I_z}{ml_f}$. The influence from $H_1(\dot{x}(t))$ on $y_p(t)$ and $\theta(t)$ by $h_1(\dot{x}(t))$ and $h_2(\dot{x}(t))$ is also quite similar.

With the help of the estimated trajectory of AGV system in Figs. 6, 7, and 8 and the estimated fault signals in Figs. 9 and 10, the controlled displacement and velocity can achieve the desired reference trajectory tracking using the proposed robust H_∞ fault-tolerant observer-based PID path tracking control strategy for AGV systems with high precision in Figs. 2, 3,

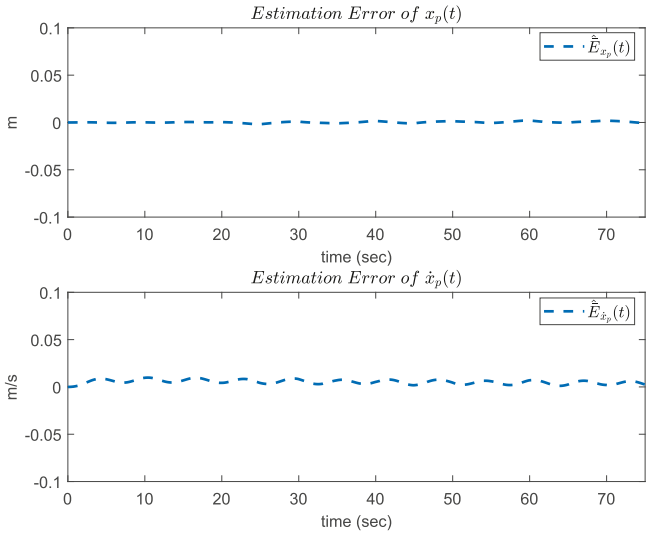

FIGURE 6. Estimated errors of longitudinal displacement $x_p(t)$ and longitudinal velocity $\dot{x}_p(t)$ by the proposed H_∞ Luenberger-type observer of AGV system in (13).

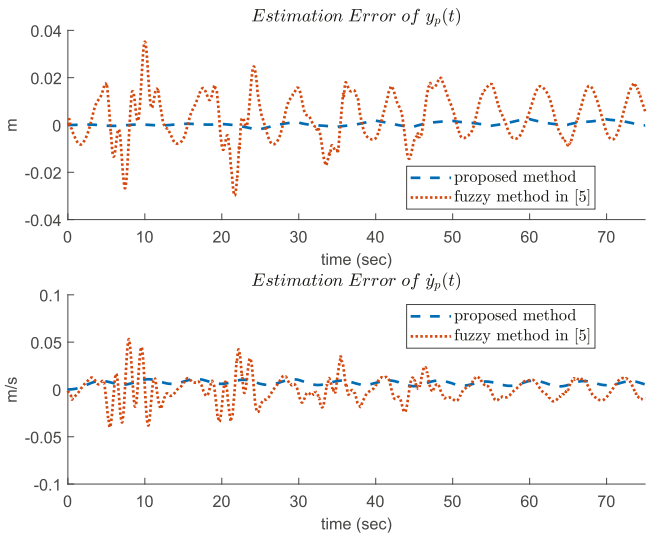

FIGURE 7. Estimated errors of lateral displacement $y_p(t)$ and lateral velocity $\dot{y}_p(t)$ by the proposed method and the fuzzy method of AGV system in [5].

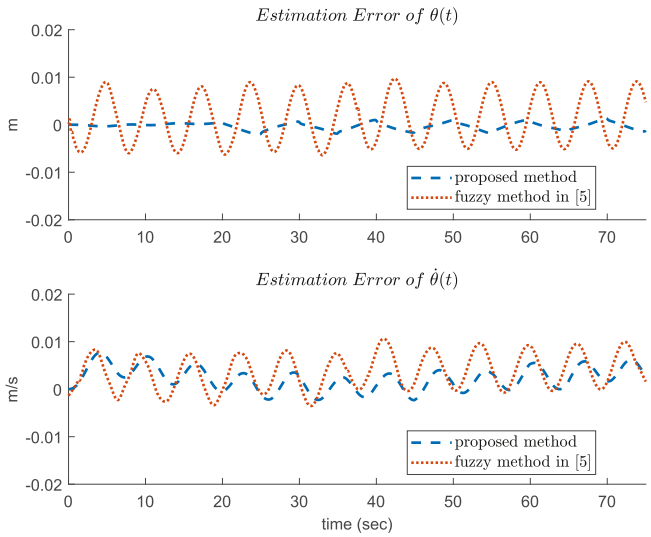

FIGURE 8. Estimated errors of yaw angle $\theta(t)$ and yaw rate $\dot{\theta}(t)$ by the proposed method and the fuzzy method of AGV system in [5].

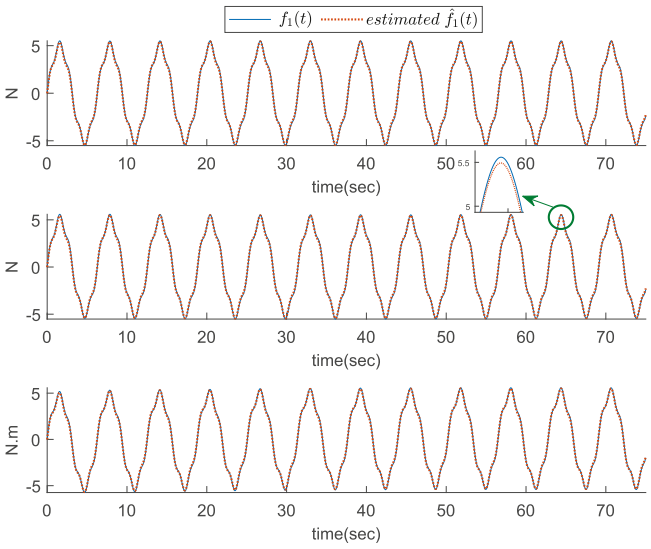

FIGURE 9. Actuator fault signal $f_1(t)$ and the corresponding estimation $\hat{f}_1(t)$.

4, and 5. By utilizing the proposed smoothed signal model, the actuator and sensor fault signals, $f_1(t)$ and $f_2(t)$, can be accurately estimated in Figs. 9 and 10 and be used for fault signal compensation via the active fault-tolerant control input $u_{PID}(t)$, as shown in Fig. 11. For instance, when the actuator fault signal $f_1(t)$ is obviously affected by the disturbance $d(t)$ and exhibits a periodic waveform in Fig. 9, the PID control $u_{PID}(t)$ in (6) also demonstrates a similar pattern but with a phase shift in Fig. 11 to compensate the influence of $f_1(t)$ on most of the controlled trajectories effectively. However, since the estimated error trajectories of AGV and the actuator/sensor fault signals are combined as the augmented system of $\bar{E}(t)$ in (13), the estimation error of the controlled trajectories of AGV system are also influenced by the estimation error of the actuator/sensor fault signals through the observer gain L in (13) by the proposed robust H_∞ fault-tolerant observer-based path tracking control strategy. Hence, the slightly larger estimation error of $f_1(t)$ and $f_2(t)$ at the peak and trough in Figs. 9 and 10 results in the periodic fluctuation in the estimation error of the system trajectories of AGV in Figs. 6, 7, and 8.

Furthermore, the robustness of proposed H_∞ fault-tolerant observer-based PID reference tracking control scheme is also demonstrated in this simulation. Even though the sensor fault signal is chosen as square wave, which may not be described as a smoothed signal at corner points, the negative effect from the approximation error on the reference tracking is efficiently attenuated by the impulse peak in the third PID control input $u_{PID,3}(t)$ and the first actual control $u_{1,1}(t)$, as shown in Figs.

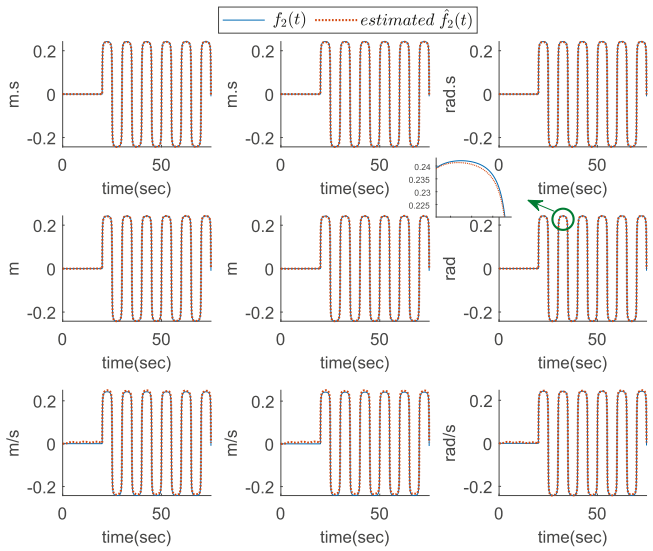

FIGURE 10. Sensor fault signal $f_2(t)$ and the corresponding estimation $\hat{f}_2(t)$.

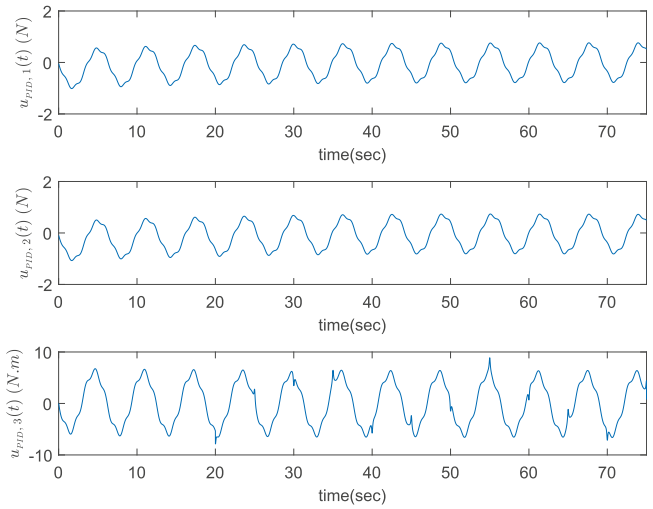

FIGURE 11. PID control $u_{PID}(t)$. From Figure 9, obviously the proposed PID control can effectively compensate the actuator fault signal.

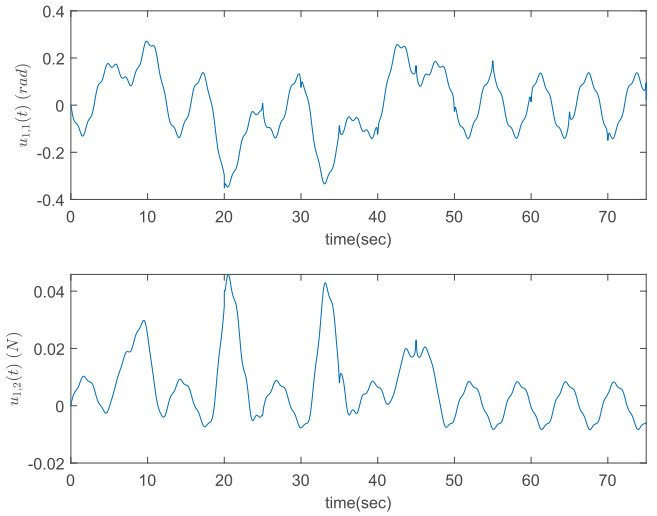

FIGURE 12. Actual control input $u_1(t) = [u_{1,1}(t)\ u_{1,2}(t)]^T$.

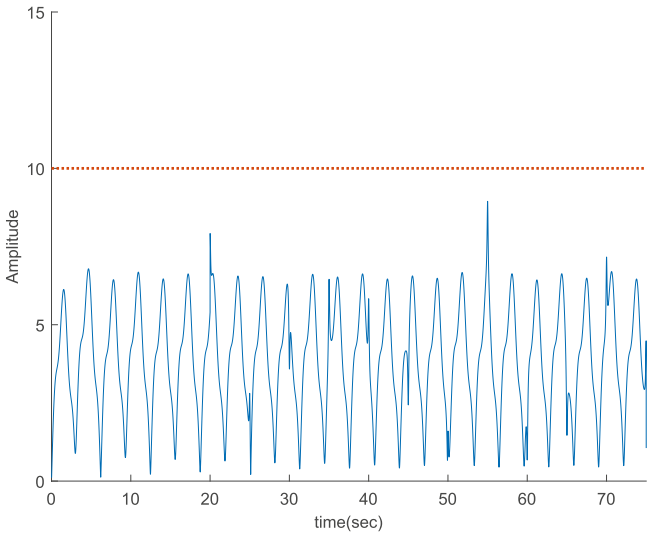

FIGURE 13. Norm of PID control input $\|u_{PID}(t)\|_2$ and the upper bound we set $\nu = 10$.

11 and 12. Such rapid impulse can be also observed in the norm of PID control input $\|u_{PID}(t)\|_2$ in Fig. 13, particularly around 5 s, 20 s and 55 s. As the result, by the proposed robust H_∞ fault-tolerant observer-based PID path reference tracking control scheme, there is no significant deviation between the trajectory of AGV and reference trajectory in Figs. 3, 4, and 5 when the sensor fault signals exhibit discontinuity in Fig. 10. Precisely, the effect of the approximation error $\tilde{v}(t)$ of the signal model on the path reference tracking error, the path estimation error and the control input is calculated as the attenuation level of $\rho = 0.1$ in (17) from the view point of energy in this simulation. The magnitude gap between the optimal attenuation level $\rho^* = 43.27$ obtained from Algorithm 1 and the actual attenuation level $\rho = 0.1$ in (17) mainly results from the conservative induced by the series inequalities in the proof of Theorem 1 and the conservative of two-step methods in (26) and (27) as well as the inequalities to obtain the actuator constraint ν in (28) and the conservative in solving the LMIs-constrained optimization problem in (29). However, the performance of the proposed optimal H_∞ fault-tolerant observer-based PID path tracking control design would be better for more practical applications of robust path tracking control of AGV system under external disturbance, measurement noise, fault signals, and actuator saturation.

On the other hand, to compare with the path tracking performance, the fuzzy robust observer-based steering control method of AGV in [5] is selected. Since the fault signals are considered as measurement noise when the robust fuzzy observer-based control strategy is designed, the simulation results of the fuzzy robust observer-based controller in [5] clearly indicate that this passive fault-tolerant control approach is less effective in dealing with both the fault signal and disturbances, leading to significant perturbations in the

estimation errors, as illustrated in Figs. 6, 7, and 8. Similar to the scenario described in the previous paragraph, the dramatic estimation errors in Figs. 7 and 8 lead to the oscillating phenomena, which are evident at 10 s, 21 s and 31 s in Figs. 4 and 5 due to the passive fault-tolerant characteristics of its observer-based control scheme. Consequently, the lateral displacement $y_p(t)$ in Fig. 4 and the yaw angle $\theta(t)$ in Fig. 5 are unable to accurately track their desired reference signals, resulting in a maximum offset of 4.8 m from the 2D trajectory in Fig. 2. In contrast, the proposed method achieves a superior path tracking performance with a maximum offset of only 0.3 m, underscoring its effectiveness.

The PID control input $u_{PID}(t)$ and the actual control input $u_1(t)$ are displayed in Figs. 11 and 12, respectively. In the presence of actuator/sensor fault signals, the PID control input $u_{PID}(t)$ exhibits a periodic waveform pattern to be served as an active fault-tolerant path tracking control mechanism. Additionally, due to the non-smoothed signal $f_2(t)$, impulse phenomena occur every 5 seconds in the third PID control input $u_{PID,3}(t)$ and the first actual control input $u_{1,1}(t)$. Besides, it is noteworthy that the magnitude of the PID control input $u_{PID}(t)$ adheres to the predefined constraint to avoid the integration of PID controller as illustrated in Fig. 13, i.e, $\|u_{PID}(t)\|_2 \leq \nu = 10$ for $t \geq 0$ which also demonstrates the effectiveness of the proposed PID control method with avoiding the actuator saturation. Even there exist rapid impulses induced by the compensation for active FTC of sensor fault signal $f_2(t)$ in Fig. 10, the amplitude of the norm of PID control input $\|u_{PID}(t)\|_2$ remains under the limit we set during designing the observer-based path tracking controller of AGV system. The actual control input $u_1(t)$ is computed using the equation $u_1(t) = G_l(\dot{x}(t))(M(\ddot{r}(t) + u_{PID}(t)) + H(\dot{r}(t)))$. Fig. 12 illustrates that despite employing $u_{PID} = \bar{K}\hat{\bar{E}}$ in the proposed control scheme, the resulting actual control inputs for the steering angle $u_{1,1}(t)$ and the brake/accelerator $u_{1,2}(t)$ after transformation remain reasonable. The variation of $u_{1,1}(t)$ at about 4 s and 41 s has larger amplitude than the variation after 50 s on positive side, which corresponds to the rotation of yaw angle when the AGV starts to switch to the left lane, while the variation starting around 18 s and 30 s has great amplitude on the opposite to match the operation for the AGV switching to the right lane too. The variation of $u_{1,2}(t)$ around these time points is also evident than other time points, which meets the braking deceleration required for AGV during turning around. This observation indicates the practical feasibility of the proposed control scheme for robust H_∞ fault-tolerant observer-based path tracking control of AGV under actuator/sensor fault signals, environmental disturbance and output measurement noise.

V. CONCLUSION

In this study, a robust H_∞ fault-tolerant observer-based PID path tracking control strategy for AGV is proposed. This strategy takes into account control saturation, measurement noise, external disturbance, and actuator/sensor fault signals to make the proposed tracking control scheme more practical. To simplify the controller design for the nonlinear AGV system and reduce the computation resource requirement in implementation, a novel path reference-based feedforward linearization method is employed. The proposed observer-based PID control scheme utilizes two smoothed signal models to effectively estimate the actuator/sensor fault signals and the system state simultaneously by the traditional Luenberger-type observer. By the proposed robust H_∞ fault-tolerant observer-based PID path tracking controller with control saturation, the robust H_∞ desired state estimation and reference path tracking performance of AGV can be achieved with the prescribed attention level ρ^2 from the energy perspective. By the proposed two-step design method, the optimal H_∞ fault-tolerant observer-based PID tracking control design problem can be transformed to a LMI-constrained optimization problem which can be solved efficiently for PID control parameters in a single round with the help of MATLAB TOOLBOX. Finally, a numerical simulation is conducted to illustrate the design procedure and validate the effective performance of the proposed Luenberger observer-based PID path tracking controller. Compared to the traditional fuzzy H_∞ passive fault-tolerant observer-based control method, the simulation results show that the AGV system can achieve a better path tracking accuracy in the triple-lane change tracking task by the proposed robust H_∞ fault-tolerant observer-based PID path tracking control strategy. Besides, both actuator and sensor fault signals can be estimated with AGV states simultaneously and can be further cancelled by PID control compensation based on the estimation of Luenberger-type observer to enhance the robust path tracking ability. Further research topic will introduce wireless network effect in the AGV network controlled system, such as package drop or input delay due to wireless channel communication, to improve the applicability.

REFERENCES

[1] S. H. Żak, *Systems and Control*. New York, NY, USA: Oxford Univ. Press, 2003.
[2] H. Zheng, W. Wu, D. Ma, and F. Qu, "Dynamic rolling horizon scheduling of waterborne AGVs for inter terminal transportation: Mathematical modeling and heuristic solution," *IEEE Trans. Intell. Transp. Syst.*, vol. 23, no. 4, pp. 3853–3865, Apr. 2022.
[3] A. Eskandarian, C. Wu, and C. Sun, "Research advances and challenges of autonomous and connected ground vehicles," *IEEE Trans. Intell. Transp. Syst.*, vol. 22, no. 2, pp. 683–711, Feb. 2021.
[4] J. Wang, Z. Luo, Y. Wang, B. Yang, and F. Assadian, "Coordination control of differential drive assist steering and vehicle stability control for four-wheel-independent-drive EV," *IEEE Trans. Veh. Technol*, vol. 67, no. 12, pp. 11453–11467, Dec. 2018.
[5] C. Zhang, J. Hu, J. Qiu, W. Yang, H. Sun, and Q. Chen, "A novel fuzzy observer-based steering control approach for path tracking in autonomous vehicles," *IEEE Trans. Fuzzy Syst.*, vol. 27, no. 2, pp. 278–290, Feb. 2019.
[6] Y. Li, K. Sun, and S. Tong, "Observer-based adaptive fuzzy fault-tolerant optimal control for SISO nonlinear systems," *IEEE Trans. Cybern.*, vol. 49, no. 2, pp. 649–661, Feb. 2019.
[7] Y. Li, S. Dong, K. Li, and S. Tong, "Fuzzy adaptive fault tolerant time-varying formation control for nonholonomic multirobot systems with range constraints," *IEEE Trans. Intell. Veh.*, vol. 8, no. 6, pp. 3668–3679, Jun. 2023.

[8] R. Marino, S. Scalzi, and M. Netto, "Nested PID steering control for lane keeping in autonomous vehicles," *Control Eng. Pract.*, vol. 19, pp. 1459–1467, 2011.

[9] H. Shen, F. Li, J. Cao, Z.-G. Wu, and G. Lu, "Fuzzy-model-based output feedback reliable control for network-based semi-markov jump nonlinear systems subject to redundant channels," *IEEE Trans. Cybern.*, vol. 50, no. 11, pp. 4599–4609, Nov. 2020.

[10] R. R. Bambulkar, G. S. Phadke, and S. Salunkhe, "Movement control of robot using fuzzy PID algorithm," in *Proc. Int. Conf. Elect. Electron. Eng. Trends Commun. Optim. Sci.*, 2016, pp. 1–5.

[11] Z. Ren, T. Zhang, X. Liu, and J. Lin, "A novel neuro PID controller of remotely operated robotic manipulators," *IEEE Trans. Circuits Syst. II-Exp. Briefs*, vol. 70, no. 6, pp. 2131–2135, Jun. 2023.

[12] D. Zhao, Z. Wang, S. Liu, Q.-L. Han, and G. Wei, "PID tracking control under multiple description encoding mechanisms," *IEEE Trans. Syst. Man, Cybern., Syst.*, vol. 53, no. 11, pp. 7025–7037, Nov. 2023.

[13] A. Al-Mayyahi, W. Wang, and P. Birch, "Path tracking of autonomous ground vehicle based on fractional order PID controller optimized by PSO," in *Proc. IEEE 13th Int. Symp. Appl. Mach. Intell. Informat.*, 2015, pp. 109–114.

[14] A. Haytham, Y. Z. Elhalwagy, A. Wassal, and N. M. Darwish, "Modeling and simulation of four-wheel steering unmanned ground vehicles using a PID controller," in *Proc. Int. Conf. Eng. Technol.*, 2014, pp. 1–8.

[15] W. Liu, M. Li, and C. Liu, "AGV dual-wheel speed synchronous control based on adaptive fuzzy PID," in *Proc. IEEE 5th Adv. Inf. Manage. Communicates Electron. Automat. Control Conf.*, 2022, pp. 564–569.

[16] D. H. Kim, "Tuning of a PID controller using an artificial immune network model and local fuzzy set," in *Proc. Joint 9th IFSA World Congr. 20th NAFIPS Int. Conf.*, 2001, pp. 2698–2703.

[17] G. Zhu, Y. Ma, and S. Hu, "Event-triggered adaptive PID fault-tolerant control of underactuated ASVs under saturation constraint," *IEEE Trans. Syst. Man, Cybern., Syst.*, vol. 53, no. 8, pp. 4922–4933, Aug. 2023.

[18] B. Verma and P. K. Padhy, "Robust fine tuning of optimal PID controller with guaranteed robustness," *IEEE Trans. Ind. Electron.*, vol. 67, no. 6, pp. 4911–4920, Jun. 2020.

[19] S. Woo, H. J. Jo, and D. H. Lee, "A practical wireless attack on the connected car and security protocol for in-vehicle CAN," *IEEE Trans. Intell. Transp. Syst.*, vol. 16, no. 2, pp. 993–1006, Apr. 2015.

[20] B. Tabbache, N. Rizoug, M. E. H. Benbouzid, and A. Kheloui, "A control reconfiguration strategy for post-sensor FTC in induction motor-based EVs," *IEEE Trans. Veh. Technol*, vol. 62, no. 3, pp. 965–971, Mar. 2013.

[21] L. Bai, Z. Gao, M. Qian, and X. Zhang, "Sliding mode observer-based FTC strategy design for satellite attitude systems with sensor fault," in *Proc. Chin. Control And Decis. Conf.*, 2019, pp. 428–433.

[22] D. Rotondo, J.-C. Ponsart, F. Nejjari, D. Theilliol, and V. Puig, "Virtual actuator-based FTC for LPV systems with saturating actuators and FDI delays," in *Proc. 3rd Conf. Control Fault-Tolerant Syst.*, 2016, pp. 831–837.

[23] Q. Shi and H. Zhang, "Fault diagnosis of an autonomous vehicle with an improved SVM algorithm subject to unbalanced datasets," *IEEE Trans. Ind. Electron.*, vol. 68, no. 7, pp. 6248–6256, Jul. 2021.

[24] W. Zhao, A. Wang, S. Zou, and H. Zhang, "Individual auxiliary and fault-tolerant control of steer-by-wire system considering different drivers steering characteristics," *IEEE/ASME Trans. Mechatronics*, vol. 26, no. 3, pp. 1558–1569, Jun. 2021.

[25] H. Deng, Y. Zhao, A.-T. Nguyen, and C. Huang, "Fault-tolerant predictive control with deep-reinforcement-learning-based torque distribution for four in-wheel motor drive electric vehicles," *IEEE/ASME Trans. Mechatronics*, vol. 28, no. 2, pp. 668–680, Apr. 2023.

[26] E. Mousavinejad, X. Ge, Q.-L. Han, T. J. Lim, and L. Vlacic, "An ellipsoidal set-membership approach to distributed joint state and sensor fault estimation of autonomous ground vehicles," *IEEE/CAA J. Autom. Sin.*, vol. 8, no. 6, pp. 1107–1118, Jun. 2021.

[27] M.-Y. Lee and B.-S. Chen, "Robust H_∞ network observer-based attack-tolerant path tracking control of autonomous ground vehicle," *IEEE Access*, vol. 10, pp. 58332–58353, 2022.

[28] B.-S. Chen and T.-W. Hung, "Integrating local motion planning and robust decentralized fault-tolerant tracking control for search and rescue task of hybrid UAVs and biped robots team system," *IEEE Access*, vol. 11, pp. 45888–45909, 2023.

[29] B.-S. Chen, M.-Y. Lee, W.-Y. Chen, and W. Zhang, "Reverse-order multi-objective evolution algorithm for multi-objective observer-based fault-tolerant control of TS fuzzy systems," *IEEE Access*, vol. 9, pp. 1556–1574, 2021.

[30] S. Boyd, L. El Ghaoui, E. Feron, and V. Balakrishnan, *Linear Matrix Inequalities in System and Control Theory*. Philadelphia, PA, USA: SIAM, 1994.

[31] B.-S. Chen, Y.-C. Liu, M.-Y. Lee, and C.-L. Hwang, "Decentralized H_∞ PID team formation tracking control of large-scale quadrotor UAVs under external disturbance and vortex coupling," *IEEE Access*, vol. 10, pp. 108169–108184, 2022.